Available online at www.sciencedirect.com
ScienceDirect
Advances in Space Research 43 (2009) 1762–1769
ADVANCES IN SPACE RESEARCH (a COSPAR publication)
www.elsevier.com/locate/asr

Variability study of the crest-to-trough TEC ratio of the equatorial ionization anomaly around 120°E longitude

Man-Lian Zhang *, Weixing Wan, Libo Liu, Baiqi Ning

Beijing National Observatory of Space Environment, Institute of Geology and Geophysics, Chinese Academy of Sciences, P.O. Box 9825, 100029 Beijing, PR China

Received 30 October 2007; received in revised form 17 September 2008; accepted 17 September 2008

Abstract

In this paper, latitudinal profiles of the vertical total electron content (TEC) deduced from the dual-frequency GPS measurements obtained at ground stations around 120°E longitude were used to study the variability of the equatorial ionization anomaly (EIA). The present study mainly focuses on the analysis of the crest-to-trough TEC ratio (TEC-CTR) which is an important parameter representing the strength of EIA. Data used for the present study covered the time period from 01 January, 1998 to 31 December, 2004. An empirical orthogonal function analysis method is used to obtain the main features of the TEC-CTR's diurnal and seasonal variations as well as its solar activity level dependency. Our results showed that: (1) The diurnal variation pattern of the TEC-CTR at 120°E longitude is characterized by two remarkable peaks, one occurring in the post-noon hours around 13–14 LT, and the other occurring in the post-sunset hours around 20–21 LT, and the post-sunset peak has a much higher value than the post-noon one. (2) Both for the north and south crests, the TEC-CTR at 120°E longitude showed a semi-annual variation with maximum peak values occurring in the equinoctial months. (3) TEC-CTR for the north crest has lower values in summer than in winter, whereas TEC-CTR for the south crest does not show this 'winter anomaly' effect. In other words, TEC-CTR for both the north and south crests has higher values in the northern hemispheric winter than in the northern hemispheric summer. (4) TEC-CTR in the daytime post-noon hours (12–14 LT) does not vary much with the solar activity, however, TEC-CTR in the post-sunset hours (19–21 LT) shows a clear dependence on the solar activity, its values increasing with solar activity.
© 2008 COSPAR. Published by Elsevier Ltd. All rights reserved.

Keywords: Low latitude ionosphere; Ionospheric variability; Equatorial ionization anomaly (EIA); GPS measurements; Total electron content (TEC)

1. Introduction

The equatorial and low latitude ionosphere is one of the most important regions of the ionosphere. It is characterized by the equatorial ionization anomaly (EIA) which has a unique structure with two crests of ionization at about ±17° dip latitude on each side of the magnetic equator and a trough in between (Appleton, 1946, 1954; see also review of Rajaram, 1977; and references therein). This equatorial ionization anomaly (EIA) phenomenon is formed as a consequence of the so called "fountain effect" which is produced by the upward ExB drift of the F region plasma and the subsequent redistribution of that plasma by a downward diffusion along the magnetic field line to a higher latitude under the influence of the gravity and the pressure gradient forces (Duncan, 1960; Stening, 1992). The electric fields that cause the uplift of the F region plasma are the electric fields created by the E and F region dynamos. Since its first discovery, EIA was extensively studied by many numerical computation/simulations and statistical analysis (e.g., Anderson, 1973; Moffett, 1979; Stening, 1992; Su et al., 1997; Walker, 1981; and references therein; Bilitza et al., 1996; Walker and Chan, 1989; Liu and Wan, 2001; Gulyaeva and Rawer, 2003; and many more).

* Corresponding author. Fax: +86 10 62010846.
E-mail address: zhangml@mail.iggcas.ac.cn (M.-L. Zhang).

0273-1177/$36.00 © 2008 COSPAR. Published by Elsevier Ltd. All rights reserved.
doi:10.1016/j.asr.2008.09.031

It has been shown by previous studies that parameters of EIA (such as the latitudinal position of the north and south crests and the amplitudes of EIA, i.e., their corresponding values of electron density Ne, the F2 peak electron density NmF2 or the total electron content, TEC) not only have diurnal variations but also depend on seasons and solar activity levels. Further more, they have north/south asymmetry and remarkable longitudinal differences, i.e., they are different for different longitudinal regions (see e.g., Walker, 1981; Bilitza et al., 1996; Su et al., 1997; Vladimer et al., 1999; Gulyaeva and Rawer, 2003; Dumin, 2002, 2007; Sagawa et al., 2005; England et al., 2006; Immel et al., 2006; Lin et al., 2007). For the East Asian region, variations of the latitudinal positions and amplitudes of EIA have been extensively studied by some authors using different dataset obtained with different measurement techniques (Walker and Poon, 1977; Walker et al., 1980, 1994; Walker and Chan, 1989; Huang et al., 1989; Huang and Cheng, 1995, 1996; Liu et al., 1999; Yeh et al., 2001; Wu et al., 2004, 2008; Tsai et al., 2001). These previous studies revealed some remarkable features of EIA in the East Asian region. For example, they found that TEC at EIA in East Asia showed mainly a semi-annual variation pattern with maximum values appearing in equinoctial months; the time of occurrence of the most developed EIA (in terms of the maximum TEC values at crest location) is earlier in winter than in summer; TEC at north crest showed winter anomaly, but no winter anomaly phenomena appeared in TEC at south crest. Statistically, TEC value at crests when EIA is most developed during the daytime has a strong and positive dependency on the solar activity level represented by proxies such as the sunspot number Rz or the 10.7 cm solar radiation flux index F10.7.

Although the variations of the latitudinal positions and amplitudes of EIA in the East Asian region have been extensively studied, the crest-to-trough ratio parameter of EIA has been less studied for this region. The crest-to-trough ratio of NmF2 or TEC can be considered as a measure of the strength of EIA which represents the development degree of EIA. It is also a measure of the strength of the fountain effect which produces the equatorial ionization anomaly. Many studies showed that the development degree of an equatorial ionization anomaly is of key importance in the generation and development of the equatorial spread F (ESF) irregularities that have important impacts on telecommunication systems. A well-developed EIA is one of the conditions conducive for the generation of ESF (Raghava Rao et al., 1988; Alex et al., 1989; Jayachandran et al., 1997) and scintillation that is most disruptive to the trans-ionospheric radiowave propagation. It occurs when an equatorial plasma bubble (EPB) intersects the maximum electron density of the equatorial anomaly. Whalen (2000, 2001, 2003, 2004) showed a close interrelationship exists between the bubble rate, the maximum pre-reversal enhancement of the *ExB* drift in the evening and the maximum electron density at crest after sunset. Moreover, it has been shown in recent years by some authors that variations of the crest-to-trough ratios of NmF2 or TEC are closely related to the generation and development of the equatorial spread F irregularities, equatorial plasma bubbles and ionospheric scintillations (Valladares et al., 2001, 2004; Henderson et al., 2005). For example, Henderson et al. (2005) using the emission line at 135.6 nm observed by TIME/GUVI, showed that for all longitudes, the crest-to-trough ratio (CTR) is well correlated with the equatorial plasma bubble rate. Some authors found that the fountain strength parameter defined as the crest-to-trough ratio in Nmax or foF2 is highly correlated with the equatorial electrojet strength (Walker and Ma, 1972; Rastogi and Klobuchar, 1990), suggesting that the crest-to-trough ratio of EIA is a parameter that can be used to study the dynamics of the equatorial ionosphere. Therefore, it is of significance to study the variability of the crest-to-trough ratio of the equatorial ionization anomaly both for scientific implication and for practical application. In this paper, we will use the vertical total electron content data derived from the GPS measurements obtained at the ground GPS receiving stations around 120°E longitude to study the variations of the crest-to-trough TEC ratios of EIA in this region.

2. Data used and analysis method

Vertical total electron contents derived by the Institute of Geology and Geophysics, CAS (IGGCAS) from the dual-frequency GPS signals are used for the present study. The derivation of vertical TEC from GPS measurements by IGGCAS is based on the assumption of single-layer (thin-shell) model of the ionosphere. Under this assumption, the slant TECs (sTEC) is converted into the vertical TEC (vTEC) on the ionospheric pierce points (IPPs) as

$$\mathrm{sTEC} = \mathrm{vTEC} \cdot M_{\mathrm{E}} + b^{\mathrm{s}} + b_{\mathrm{r}} \quad (1)$$

where $M_{\mathrm{E}} = 1/\cos(\chi)$ is the mapping function, χ is the zenith angle of GPS satellite at the single layer height of the ionosphere, b^{s} and b_{r} are the instrument biases of the satellites and receivers, respectively. Then the vertical TECs (vTEC) at grids and the instrument biases b^{s} and b_{r} are obtained by combining interpolation and least-square fitting procedure. For details of the method used to derive the vTECs from GPS measurements, please refer to Mao (2007) and Mao et al. (2008).

In this study, we use the vertical TEC data with half hour time resolution for the 120°E longitude and at latitudinal grids with every 2.5° from 40°S to 60°N geographical latitudes that are derived from the GPS dual-frequency measurements observed during the period 1996–2004 at (1) China Network stations; (2) South-East Asian stations and (3) Australian stations. Due to the data quality problem for the years 1996 and 1997, only data for the years of 1998–2004 are used for the present study.

The latitudinal profiles of the vertical TEC at 120°E longitude at every hour interval are extracted, then for each TEC latitudinal profile, the latitudinal positions of the

crests and trough and their corresponding TEC values are found with the help of a specially developed software that can be controlled manually when picking up the latitudinal positions of the EIA's crests and trough. TEC values at the crests and trough are obtained by interpolation. The crest-to-trough TEC ratios are then calculated after the TEC values at crests and trough are found.

An eigen mode analysis is then applied to the crest-to-trough TEC ratio dataset obtained above. The eigen mode analysis method decomposed the dataset into the sum of a series of orthogonal base functions E_i representing the diurnal variation of the dataset, multiplied by the associated coefficients A_i representing the longer period (day-to-day, seasonal and solar cycle) variations (Liu et al., 2007):

$$\text{TEC-CTR}(t,d) = \sum E_i(t) * A_i(d)$$

where t is time (universal time or local time) representing diurnal changes, d is day number counted consecutively starting from 01 January, 1998 to 31 December, 2004. The eigen mode base functions E_i and the associated coefficients A_i are determined directly by the dataset itself during calculation procedure. For this reason, this method is also called the empirical orthogonal function (EOF) analysis method. EOF analysis method has the advantage that the base functions E_i and the associated coefficients A_i determined possess the intrinsic characteristics of the original dataset and the eigen series converges quickly. This makes it possible to capture most of the variances of a dataset using only a few orders of EOF components.

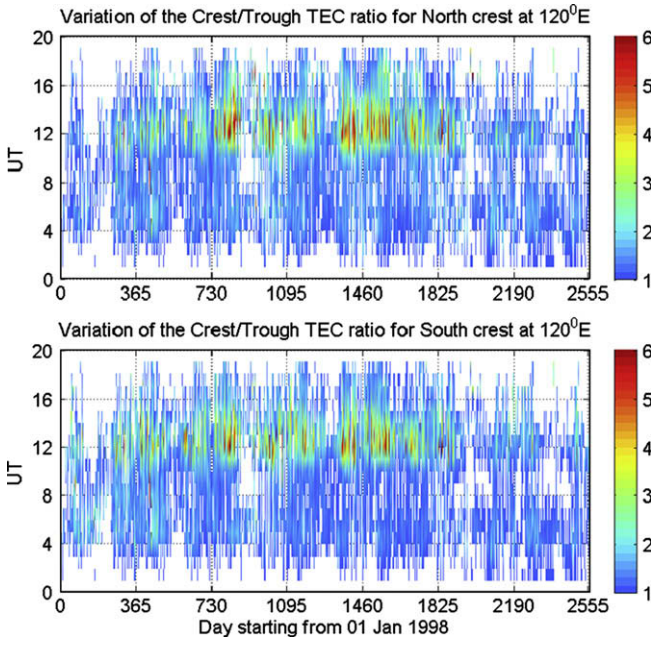

Fig. 1. Contour plots of the crest-to-trough TEC ratios of EIA at 120°E versus universal time (UT) and day during 01 Jan 1998 to 31 December 2004.

3. Results

Fig. 1 shows the variations of the crest-to-trough TEC ratios (hereafter referred to as TEC-CTR) versus the universal time (UT) and the days counted consecutively from 01 January, 1998 to 31 December, 2004. The upper panel in Fig. 1 is for the north crest of EIA and the lower panel for the south one. Please note that there is an 8-h difference between the local time (LT) at 120°E and the universal time (UT): LT = UT + 8. From Fig. 1, it can be seen that both for the north and south crests of EIA, the most remarkable features for the diurnal variation of TEC-CTR are the two peak values, one occurring in the post-noon hours around 5–6 UT (13–14 LT), and the other occurring in the post-sunset hours around 12–13 UT (20–21 LT). This can be seen more clearly in Figs. 2 and 3 that show the statistical plots month by month of the diurnal variation of the TEC-CTR at 120°E longitude for the high solar activity year 2001 and the low solar activity year 2004, respectively. Note that in Figs. 2 and 3, the TEC-CTR for the south crest is plotted as negative value for distinguishing it from that for the north crest. It can be seen that the post-sunset peak has a much higher value than the post-noon one. Generally, the value of TEC-CTR is seldom larger than 2 during the daytime hours, but during the nighttime hours, in particular for the post-sunset hours, quite often it is larger than 2 and can be much higher than 2. This enhancement of TEC-CTR after sunset must be resulted from the regeneration/enhancement of the fountain effect responsible for the formation of the crest and trough structure of EIA in the equatorial and low latitude region. The regeneration/enhancement of the fountain effect during the post-sunset hours is due to the evening pre-reversal enhancement of the F2 region plasma's electromagnetic ExB drift due to the enhanced zonal electric field near the magnetic equator (Fejer et al., 1995; and references therein). Carefully inspecting the diurnal variation of TEC values at crests and trough (plots not shown here), it is found that although the TEC at EIA's crests during the post-sunset hours is only slightly enhanced or even just the decay rate of it is slowed down, TEC at EIA's trough is much more reduced (with a much faster decay rate) during this post-sunset hours, resulting in the large enhancement of the crest-to-trough TEC ratios. This confirms that the post-sunset enhancement of TEC-CTR is due to the regeneration/enhancement of the fountain effect after sunset. This regeneration/enhancement of the EIA strength or the fountain strength after sunset is particularly strong for the equinoctial months during the high solar activity years.

For the seasonal variation, it is observed that the TEC-CTR shows mainly a semi-annual variation pattern, with both the post-noon and post-sunset peaks reaching maximum values in the equinoctial months and this semi-annual variation pattern is true for both the north and south crests. These seasonal variation features can be seen clearly from Figs. 1 to 3. It is also observed that TEC-CTRs both for north and south crests reach minimum values at north

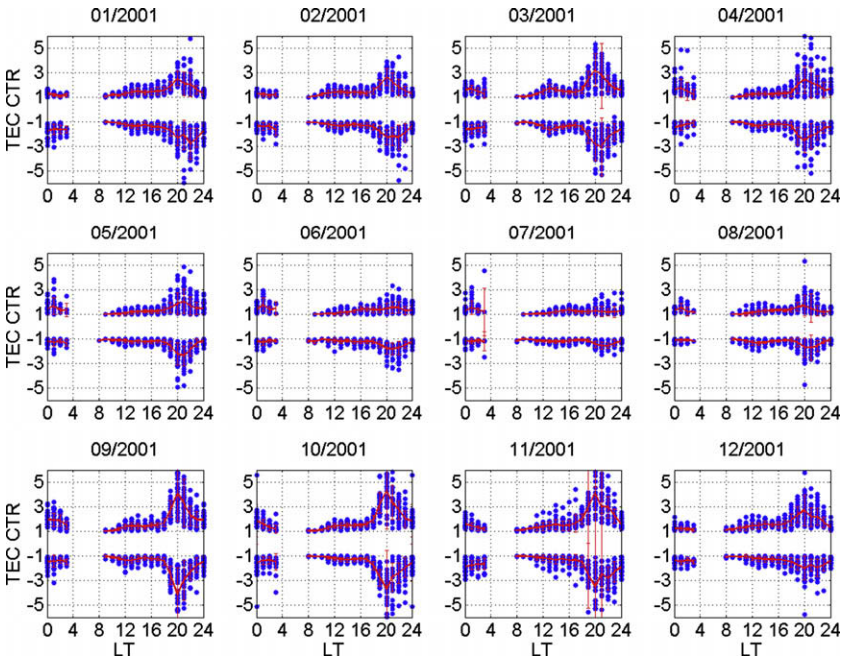

Fig. 2. Diurnal variation of the crest-to-trough TEC ratios of EIA at 120°E for the 12 months of the year 2001. Note that the crest-to-trough TEC ratio for south crest is plotted as negative value for distinguishing it from that for north crest.

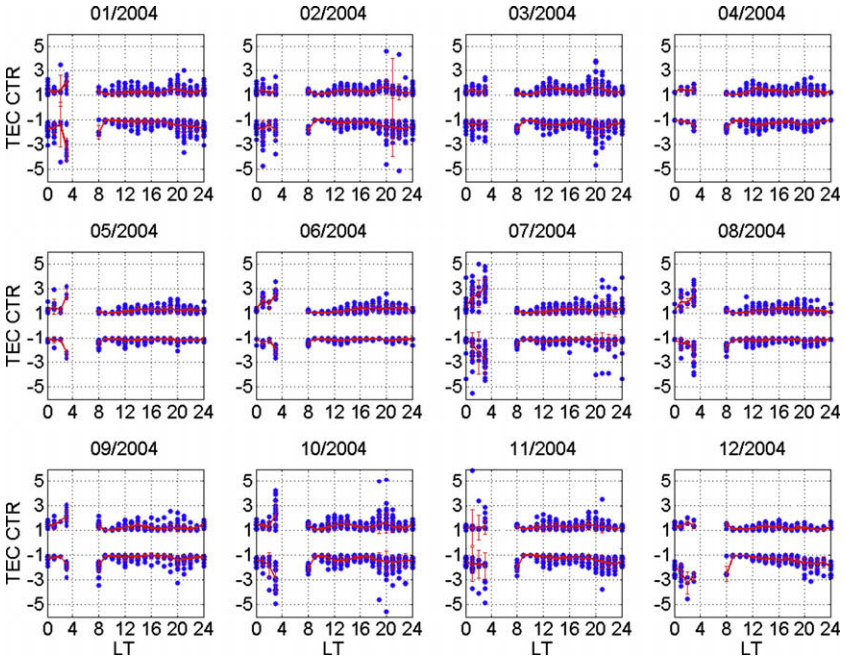

Fig. 3. Diurnal variation of the crest-to-trough TEC ratios of EIA at 120°E for the 12 months of the year 2004. Note that the crest-to-trough TEC ratio for south crest is plotted as negative value for distinguishing it from that for north crest.

hemispheric summer months around June and July. In other words, TEC-CTR for the north crest has a larger value in winter than in summer, whereas TEC-CTR for the south crest does not show this 'winter anomaly' effect. Usually, when talking about 'winter anomaly', the parameter NmF2 (the F2 peak electron density) or TEC is concerned. The 'winter anomaly' of NmF2 (the F2 peak electron density) or TEC itself is largely a neutral composition effect resulted from the global thermospheric circulation and is a phenomena mainly prevailing at middle latitudes in particular for north hemisphere (Pavlov and Pavlova, 2005a,b; Rishbeth et al., 2000; and references therein). Therefore there is hemispheric difference. In this paper, we are discussing the crest-to-trough TEC ratio in the equatorial anomaly region. This ratio is a measure of the equatorial anomaly's strength that is more closely

related to the strength of the fountain effect that depends on the equatorial plasma's vertical drift driven by the electric field. According to the observations of AE-E satellite (see Fig. 2 in Fejer et al., 1995), in average the post-sunset equatorial upward drift induced by electric field is higher in northern winter than in northern summer in particular for the high solar flux condition. As a result, it is understandable that the ratio peaks behavior simultaneously in both hemispheres: this is a result of a common driver – electric fields.

We have conducted an EOF analysis to the crest-to-trough TEC ratio dataset. As described at the end of Section 2, in our EOF analysis, we decomposed the dataset into the base functions E_i representing diurnal variation and the associated coefficients A_i representing seasonal and solar cycle variations. It is found that for TEC-CTR, the first order component of EOF decomposition can explain most (~80%) of the variances of the dataset. It represents the main characteristics of TEC-CTR which can be considered as the climatologically variation of TEC-CTR. The rest variations are explained by the higher order of EOF components that mainly reflects more complicated irregular day-to-day variability of TEC-CTR. Fig. 4 shows the variation patterns of the first order eigen function E_1 (upper panel) and the associated coefficient A_1 (lower panel) of the EOF analysis result. Note that E_1 and A_1 for the south crest are plotted as negative values for distinguishing from those for the north crest. Black solid lines in the lower panel in Fig. 4 are the 27-day smoothed values of A_1. It can be seen that the results obtained by the EOF analysis are consistent with what we have described above on the diurnal and seasonal variations patterns of the crest-to-trough TEC ratios. By the nature of EOF analysis (and also by our experience), the first order component of the EOF analysis (E_1, A_1) will capture the main intrinsic characteristics of the dataset analyzed. Hence, E_1 reflects the main intrinsic characteristic diurnal variation embedded in the dataset and A_1 reflects the main intrinsic characteristic seasonal and solar cycle variations embedded in the dataset. Indeed, as shown in the upper panel of Fig. 4, the variation of E_1 with local time does show features such as the two peaks (one around 13–14 LT and the other around 20 LT) that are the most remarkable diurnal variation pattern of the crest-to-trough ratio seen in Fig. 1.

Figs. 5 and 6 show the scatter plots month by month of the crest-to-trough TEC ratios, averaged for 12–14 LT and 19–21 LT time bins, respectively, versus the F10.7 index. These two time bins are selected because they correspond to the two periods when the crest-to-trough TEC ratios reach peak values during the diurnal variation procedure. It can be seen that the dependence of the ratio on solar activity is different for the two time bins. For the 12–14 LT time bin, the ratio does not vary much with F10.7, whereas for the 19–21 LT time bin, the ratio shows a clear dependence on the solar activity, its values increasing with solar activity. These different behaviors for the two time bins may be explained as follows. As is well known, the equatorial ionization anomaly is formed by the fountain effect caused by the upward vertical drifts of the equatorial plasma due to electric field, followed by redistribution of that plasma by a downward diffusion along the magnetic field line to higher latitudes under the influence of the gravity and the pressure gradient forces. However, the two peaks of the crest-to-trough TEC ratio in the diurnal variation procedure are due to electric fields originating from totally different mechanisms. The post-noon one is related to the electric field created by the daytime E region dynamo, whereas the post-sunset one is caused by the elec-

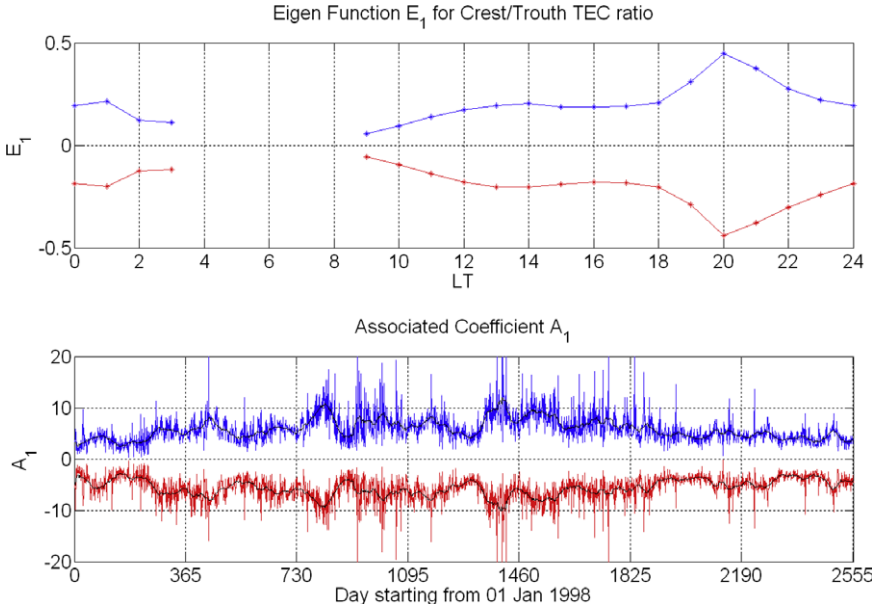

Fig. 4. Plots of the first order eigen function E_1 (upper panel) and the associated EOF coefficient A_1 (lower panel) for the crest-to-trough TEC ratios of EIA at 120°E. Note that E_1 and A_1 for the south crest are plotted as negative values for distinguishing from those for north crest.

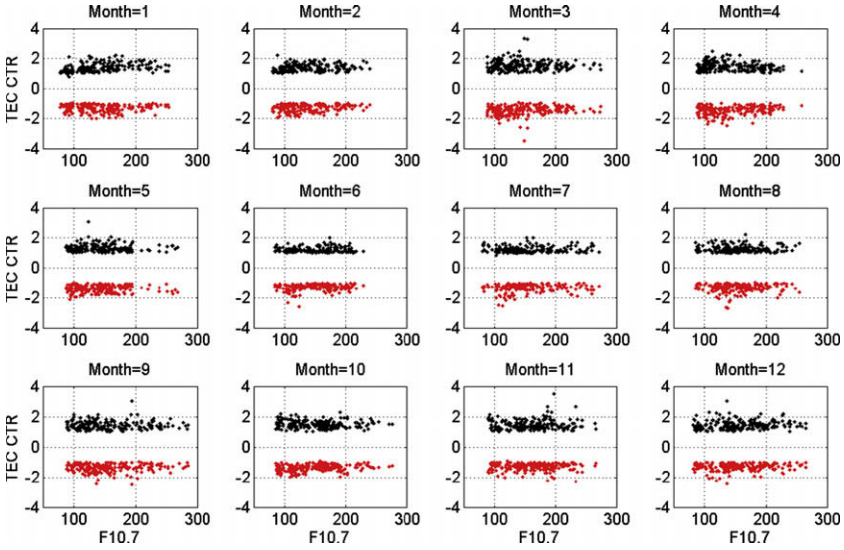

Fig. 5. Scatter plots of crest-to-trough TEC ratio versus F10.7 for the 12–14 LT time bin. Note that results for the south crest are plotted as negative values for distinguishing from those for north crest.

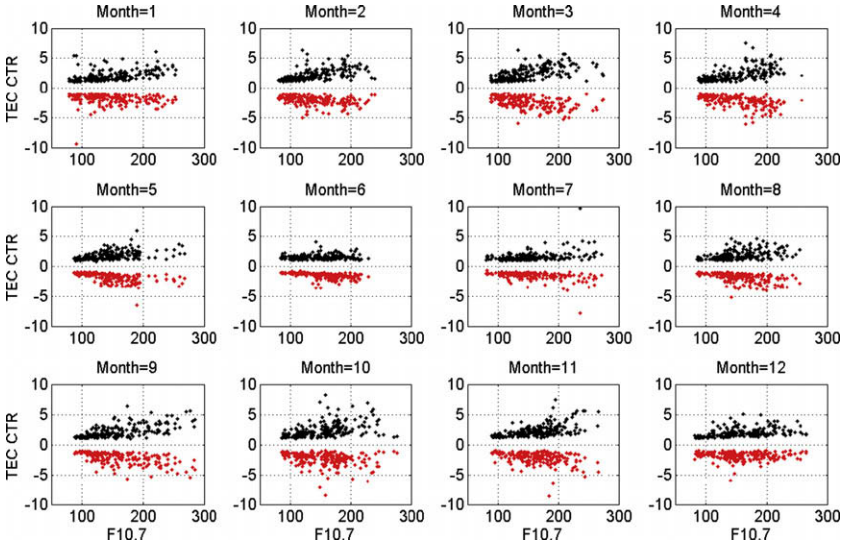

Fig. 6. Scatter plots of crest-to-trough TEC ratio versus F10.7 for the 19–21 LT time bin. Note that results for the south crest are plotted as negative values for distinguishing from those for north crest.

tric field mostly related with the F region dynamo that takes effect after sunset (Farley et al., 1986). Since the crest-to-trough TEC ratio is a measure of the equatorial anomaly's strength, it should be closely related to the strength of the fountain effect that depends on the equatorial plasma's vertical drifts induced by the electric fields. According to Fejer and Scherliess (2001), the daytime average upward equatorial F-region vertical drift caused by electric field do not vary much with solar activity, but the evening upward drifts increase from solar minimum to solar maximum. This behavior of the dependence of the equatorial F-region vertical drifts on the solar activity causes a similar solar activity dependency of the crest-to-trough TEC ratio in the equatorial anomaly region.

4. Summary and conclusions

In the present study, latitudinal profiles of the vertical total electron content (TEC) deduced from the dual-frequency GPS measurements that are obtained at the ground stations around 120°E longitude during the time period of 1998–2004 were used to study the variability of the EIA's strength parameter defined as the crest-to-trough TEC ratio. An empirical orthogonal function analysis method is used to obtain the main features of the TEC-CTR's diurnal and seasonal variations as well as their solar activity level dependency. Our results showed that: (1) The diurnal variation pattern of the TEC-CTR at 120°E longitude is characterized by two remarkable peaks, one occurring in

the post-noon hours around 13–14 LT, and the other occurring in the post-sunset hours around 20–21 LT, and the post-sunset peak has a much higher value than the post-noon one. This means that in terms of the crest-to-trough TEC ratio, EIA reaches its largest strength in the post-sunset hours before midnight, implying that EIA is regenerated/enhanced during these post-sunset hours. This is particularly true for the equinoctial months during the high solar activity years. (2) Both for the north and south crests, the TEC-CTR at 120°E longitude showed a semi-annual variation with maximum peak values occurring in the equinoctial months. (3) TEC-CTR for the north crest has lower values in summer than in winter, whereas TEC-CTR for the south crest does not show this 'winter anomaly'. In other words, both the TEC-CTR for the north and south crests has higher values in the north hemispheric winter around December–January months than in the north hemispheric summer around June–July months. This might be a result of a common driver – electric fields. (4) TEC-CTR in the daytime post-noon hours (12–14 LT) does not vary much with the solar activity, however, TEC-CTR in the post-sunset hours (19–21 LT) shows a clear dependence on the solar activity, its values increasing with solar activity. This is due to the similar dependence of the equatorial F-region vertical drifts on the solar activity.

Acknowledgements

This research was supported by the National Natural Science Foundation of China (40774092, 40636032) and the National Important Basic Research Project (2006CB806306).

References

Alex, S., Koparkar, P.V., Rastogi, R.G. Spread-F and ionization anomaly belt. J. Atmos. Terr. Phys. 51, 371–379, 1989.

Anderson, D.N. A theoretical study of the ionospheric F region equatorial anomaly–I. Theory. Planet. Space Sci. 21, 409–419, 1973.

Appleton, E.V. Two anomalies in the ionosphere. Nature 157, 691–693, 1946.

Appleton, E.V. The anomalous equatorial belt in the F2-layer. J. Atmos. Terr. Phys. 5, 348–351, 1954.

Bilitza, D., Koblinsky, C., Zia, S., Williamson, R., Beckley, B. The equatorial anomaly region as seen by the Topex/Poseidon satellite. Adv. Space Res. 18 (6), 23–32, 1996.

Dumin, Y.V. Global structure of longitudinal variations in the equatorial anomaly of ionospheric F2-layer. Adv. Space Res. 29 (6), 907–910, 2002.

Dumin, Y.V. The accuracy of IRI in the description of development of the equatorial (Appleton) anomaly. Adv. Space Res. 39 (5), 687–690, 2007.

Duncan, R.A. The equatorial F region of the ionosphere. J. Atmos. Terr. Phys. 18 (2), 89–100, 1960.

England, S.L., Immel, T.J., Sagawa, E., Henderson, S.B., Hagan, M.E., Mende, S.B., Frey, H.U., Swenson, C.M., Paxton, L.J. Effect of atmospheric tides on the morphology of the quiet time, postsunset equatorial ionospheric anomaly. J. Geophys. Res. 111, A10S19, doi:10.1029/2006JA011795, 2006.

Farley, D.T., Bonelli, E., Fejer, B.G., Larsen, M.F. The prereversal enhancement of the zonal electric field in the equatorial ionosphere. J. Geophys. Res. 91, 13723–13728, 1986.

Fejer, B.G., de Paula, E.R., Heelis, R.A., Hanson, W.B. Global equatorial ionospheric vertical plasma drifts measured by the AE-E satellite. J. Geophys. Res. 100 (4), 5769–5776, 1995.

Fejer, B.G., Scherliess, L. On the variability of equatorial F-region vertical plasma drifts. J. Atmos. Terr. Phys. 63 (9), 893–897, 2001.

Gulyaeva, T.L., Rawer, K. North/south asymmetry of the equatorial anomaly: a model study. Adv. Space Res. 31 (3), 549–554, 2003.

Henderson, S.B., Swenson, C.M., Christensen, A.B., Paxton, L.J. Morphology of the equatorial anomaly and equatorial plasma bubbles using image subspace analysis of Global Ultraviolet Imager data. J. Geophys. Res. 110, A11306, doi:10.1029/2005JA011080, 2005.

Huang, Y.-N., Cheng, K., Chen, S.W. On the equatorial anomaly of the ionospheric total electron content near the northern anomaly crest region. J. Geophys. Res. 94, 13515–13525, 1989.

Huang, Y.-N., Cheng, K. Solar cycle variation of the total electron content around equatorial anomaly crest region in East Asia. J. Atmos. Terr. Phys. 57 (12), 1503–1511, 1995.

Huang, Y.-N., Cheng, K. Solar cycle variations of the equatorial ionospheric anomaly in total electron content in Asian region. J. Geophys. Res. 101 (A11), 24513–24520, 1996.

Immel, T.J., Sagawa, E., England, S.L., Henderson, S.B., Hagan, M.E., Mende, S.B., Frey, H.U., Swenson, C.M., Paxton, L.J. Control of equatorial ionospheric morphology by atmospheric tides. Geophys. Res. Lett. 33, L15108, doi:10.1029/2006GL026161, 2006.

Jayachandran, P.T., Sri Ram, P., Somayajulu, Y.V., Rama Rao, P.V.S. Effect of equatorial ionization anomaly on the occurrence of spread-F. Ann. Geophys. 15, 255–262, 1997.

Lin, C.H., Wang, W., Hagan, M.E., Hsiao, C.C., Immel, T.J., Hsu, M.L., Liu, J.Y., Paxton, L.J., Fang, T.W., Liu, C.H. Plausible effect of atmospheric tides on the equatorial ionosphere observed by the FORMOSAT-3/COSMIC: three-dimensional electron density structures. Geophys. Res. Lett. 34, L11112, doi:10.1029/2007GL029265, 2007.

Liu, C., Zhang, M.-L., Wan, W., Liu, L., Ning, B. Modeling M(3000)F2 based on empirical orthogonal function analysis method. Radio Sci. 43, RS1003, doi:10.1029/2007RS003694, 2007.

Liu, J.Y., Tsai, H.F., Wu, C.C., Tseng, C.L., Tsai, L.C., Tsai, W.H., Liou, K., Chao, J.K. The effect of geomagnetic storm on ionospheric total electron content at the equatorial anomaly region. Adv. Space Res. 24 (11), 1491–1494, 1999.

Liu, L., Wan, W. The evolution of equatorial trough of ionospheric F-region ionization. Terr. Atmos. Ocean. Sci. 12 (3), 559–565, 2001.

Mao, T. Nowcasting and Modeling the Ionospheric TEC from the Observation of GPS Network, Ph.D Thesis. Institute of Geology and Geophysics, Chinese Academy of Sciences, 2007.

Mao, T., Wan, W., Yue, X., Sun, L., Zhao, B., Guo, J. An empirical orthogonal function model of total electron content over China. Radio Sci., doi:10.1029/2007RS003629, 2008.

Moffett, R.J. The equatorial anomaly in the electron distribution of the Terrestrial F-region. Fundam. Cosmic Phys. 4, 313–391, 1979.

Pavlov, A.V., Pavlova, N.M. Causes of the mid-latitude NmF2 winter anomaly at solar maximum. J. Atmos. Terr. Phys. 67, 862–877, 2005a.

Pavlov, A.V., Pavlova, N.M. Causes of the mid-latitude NmF2 winter anomaly at solar maximum. J. Atmos. Terr. Phys. 67, 862–877, 2005b.

Rajaram, G. Structure of the equatorial F-region, topside and bottomside – a review. J. Atmos. Terr. Phys. 39, 125–1144, 1977.

Raghava Rao, R., Nageswara Rao, M., Sastri, J.H., Vyas, G.D., Srirama Rao, M. Role of equatorial ionization anomaly in the initiation of equatorial spread-F. J. Geophys. Res. 93, 5959–5964, 1988.

Rastogi, R.G., Klobuchar, J.A. Ionospheric electron content within the equatorial F2 layer anomaly belt. J. Geophys. Res. 95 (A11), 19045–19052, 1990.

Rishbeth, H., Muller-Wodarg, I.C.F., Zou, L., Fuller-Rowell, T.J., Millward, G.H., Moffett, R.J., Idenden, D.W., Aylward, A.D. Annual and semiannual variations in the ionospheric F2-layer: II. Physical discussion. Ann. Geophys. 18, 945–956, 2000.

Sagawa, E., Immel, T.J., Frey, H.U., Mende, S.B. Longitudinal structure of the equatorial anomaly in the nighttime ionosphere observed by

IMAGE/FUV. J. Geophys. Res. 110, A11302, doi:10.1029/2004JA010848, 2005.

Stening, R.J. Review paper: modelling the low latitude F region. J. Atmos. Terr. Phys. 54, 1387–1421, 1992.

Su, Y.Z., Bailey, G.J., Oyama, K.I., Balan, N. A modelling study of the longitudinal variations in the north-south asymmetries of the ionospheric equatorial anomaly. J. Atmos. Terr. Phys. 59 (11), 1299–1310, 1997.

Tsai, H.F., Liu, J.Y., Tsai, W.H., Liu, C.H., Tseng, C.L., Wu, C.-C. Seasonal variations of the ionospheric total electron content in Asian equatorial anomaly regions. J. Geophys. Res. 106 (A12), 30363–30370, 2001.

Valladares, C.E., Basu, S., Groves, K., Hagan, M.P., Hysell, D., Mazzella Jr., A.J., Sheehan, R.E. Measurements of the latitudinal distributions of total electron content during equatorial spread F events. J. Geophys. Res. 106 (A12), 29133–29152, 2001.

Valladares, C.E., Villalobos, J., Sheehan, R., Hagan, M.P. Latitudinal extension of low-latitude scintillations measured with a network of GPS receivers. Ann. Geophys. 22, 3155–3175, 2004.

Vladimer, J.A., Jastrzebski, P., Lee, M.C., Doherty, P.H., Decker, D.T., Anderson, D.N. Longitude structure of ionospheric total electron content at low latitudes measured by the TOPEX/Poseidon satellite. Radio Sci. 34 (5), 1239–1260, 1999.

Walker, G.O., Ma, J.H.K. Influence of solar flux and the equatorial electrojet on the diurnal development of the latitude distribution of total electron content in the equatorial anomaly. J. Atmos. Terr. Phys. 34 (8), 1419–1424, 1972.

Walker, G.O. Longitudinal structure of the F-region equatorial anomaly – a review. J. Atmos. Terr. Phys. 43 (8), 763–774, 1981.

Walker, G.O., Ma, J.H.K., Golton, E. The equatorial ionospheric anomaly in electron content from solar minimum to solar maximum for South East Asia. Ann. Geophys. 12, 195–209, 1994.

Walker, G.O., Chan, H.F. Computer simulations of the seasonal variation of the ionospheric equatorial anomaly in East Asia under solar minimum conditions. J. Atmos. Terr. Phys. 51, 953–974, 1989.

Walker, G.O., Poon, C.B. The early morning development and the evening decay of electron content-latitude profiles at low latitudes and their dependence upon solar declination. J. Atmos. Terr. Phys. 39 (9–10), 1145–1154, 1977.

Walker, G.O., Ma, J.H.K., Rastogi, R.G., Deshpande, M.R., Chakdra, H. Dissimilar forms of the ionospheric equatorial anomaly observed in East Asia and India. J. Atmos. Terr. Phys. 42 (7), 629–635, 1980.

Whalen, J.A. An equatorial bubble: its evolution observed in relation to bottom side spread F and to the Appleton anomaly. J. Geophys. Res. 105 (A3), 5303–5315, 2000.

Whalen, J.A. The equatorial anomaly: Its quantitative relation to equatorial bubbles, bottomside spread F, and ExB drift velocity during a month at solar maximum. J. Geophys. Res. 106 (A12), 29125–29132, 2001.

Whalen, J.A. Dependence of the equatorial anomaly and of equatorial spread F on the maximum prereversal ExB drift velocity measurement. J. Geophys. Res. 108 (A5), 1193, doi:10.1029/2002JA009755, 2003.

Whalen, J.A. Linear dependence of the postsunset equatorial anomaly electron density on solar flux and its relation to the maximum prereversal ExB drift velocity through its dependence on solar flux. J. Geophys. Res. 109, A07309, doi:10.1029/2004JA010528, 2004.

Wu, C.C., Fryb, C.D., Liuc, J.-Y., Lioud, K., Tseng, C.-L. Annual TEC variation in the equatorial anomaly region during the solar minimum: September 1996–August 1997. J. Atmos. Terr. Phys. 66, 199–207, 2004.

Wu, C.C., Liou, K., Shan, S.-J., Tseng, C.-L. Variation of ionospheric total electron content in Taiwan region of the equatorial anomaly from 1994 to 2003. Adv. Space Res. 41 (2008), 611–616, doi:10.1016/j.asr.2007.06.013, 2008.

Yeh, K.C., Franke, S.J., Andreeva1, E.S., Kunitsyn, V.E. An investigation of motions of the equatorial anomaly crest. Geophys. Res. Lett. 28 (24), 4517–4520, 2001.